ELSEVIER

Materials Science and Engineering A319–321 (2001) 597–601

MATERIALS SCIENCE & ENGINEERING A

www.elsevier.com/locate/msea

Foreign-object damage and high-cycle fatigue of Ti–6Al–4V

J.O. Peters, R.O. Ritchie *

Department of Materials Science and Engineering, University of California, Berkeley, CA 94720-1760, USA

Abstract

Recent high-cycle fatigue (HCF) related failures of gas-turbine jet engines have prompted a re-examination of the design methodologies for HCF-critical components, such as titanium alloy turbine blades. As foreign-object damage (FOD) from ingested debris is a key concern for HCF-related failures of such blades, the current study is focused on the role of simulated high velocity FOD in affecting the initiation and early growth of small surface fatigue cracks in a Ti–6Al–4V alloy, processed for typical blade applications. It is found that resistance to HCF is markedly reduced, primarily due to earlier fatigue crack initiation. The mechanistic effect of FOD on such premature fatigue crack initiation and the subsequent crack growth is discussed in terms of four prominent factors: (i) the presence of small microcracks in the damaged zone; (ii) the stress concentration associated with the FOD indentation; (iii) the localized presence of tensile residual hoop stresses at the base and rim of the indent sites; and (iv) microstructural damage from FOD-induced plastic deformation. In view of the in-service conditions, i.e., small crack sizes, high frequency (>1 kHz) vibratory loading and (depending on the blade span location) high mean stress levels, a damage-tolerant design approach, based on the concept of a threshold for no fatigue-crack growth, appears to offer a preferred solution. It is shown that FOD-initiated cracks that are of a size comparable with microstructural dimensions can propagate at applied stress-intensity ranges on the order of $\Delta K \sim 1$ MPa$\sqrt{\text{m}}$.

Keywords: Foreign-object damage; High-cycle fatigue (HCF); Fatigue-crack growth threshold; Small cracks; Ti–6Al–4V

1. Introduction

The increasing incidence of high-cycle fatigue (HCF)-related titanium alloy fan and compressor blade failures in military gas-turbine engines, involving (i) foreign-object damage; (ii) fretting and (iii) interactions of low cycle fatigue (LCF) and HCF loading, has instigated a re-examination of the current Goodman design approach for HCF [1,2]. Indeed, design against HCF, based on a damage-tolerant concept of a fatigue-crack growth threshold for no cracking, would appear to offer a preferred approach. However, such thresholds have to reflect representative HCF conditions of high frequencies, small crack sizes and, depending on the blade span location, very high mean stress levels [1,2].

Foreign-object damage (FOD), from hard body impacts such as stones, which impact primarily on the fan blades, can result in immediate blade fracture or damage from stress-raising notches [3,4] or cracks [5], depending on the severity of impact. In a recent study on Ti–6Al–4V [5], where such damage was simulated by high-velocity impacts of steel shot on a flat surface, FOD was found to markedly reduce the fatigue strength. It was observed that small microcracks formed in the damaged region of the highest velocity impacts (300 m s^{-1}), and provided preferred sites for premature fatigue crack initiation on subsequent fatigue cycling. In general, these mechanistic effects can be described in terms of (i) FOD-induced microcracks in the damage zone, (ii) stress concentration associated with the FOD-indentation, (iii) localized presence of impact induced tensile residual hoop stresses at locations of the preferred sites for crack initiation, and (iv) microstructural damage from FOD-induced plastic deformation.

In the present study, we further investigate the effect of FOD-induced microcracks (~ 2–10 μm) at an impact velocity of 300 m s^{-1} in a Ti–6Al–4V alloy, $\alpha+\beta$ processed for turbine blade applications. Specifically, the threshold conditions for fatigue crack initiation and growth of such microcracks are defined and compared

* Corresponding author. Tel.: +1-510-486-5798; fax: +1-510-486-4995.

E-mail address: roritchie@lbl.gov (R.O. Ritchie).

0921-5093/01/$ - see front matter
PII: S0921-5093(01)00982-0

with the fatigue threshold (ΔK_{TH}) behavior of naturally-initiated small ($2c \sim 45$–1000 μm) and large through-thickness (>5 mm) cracks in undamaged material.

2. Experimental procedures

The titanium alloy Ti–6Al–4V under study (chemical composition Ti–6.30Al–4.19V–0.19Fe–0.19O, wt.%), was from the forgings produced for U.S. Air Force sponsored programs on High-Cycle Fatigue. Material and processing details are given in [5]. The bimodal microstructure is shown in Fig. 1. Uniaxial tensile tests (performed parallel to the plate length), gave a yield stress of 915 MPa, UTS of 965 MPa and tensile elongation of 19%. Foreign-object damage was simulated by firing 3.2 mm Cr-hardened steel spheres, normally onto a flat specimen surface of uniaxial fatigue

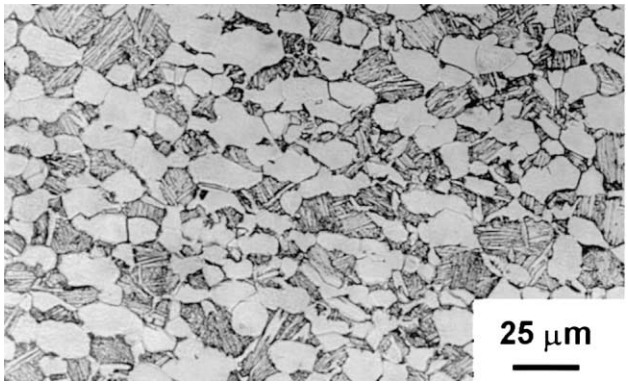

Fig. 1. Bimodal microstructure of Ti–6Al–4V.

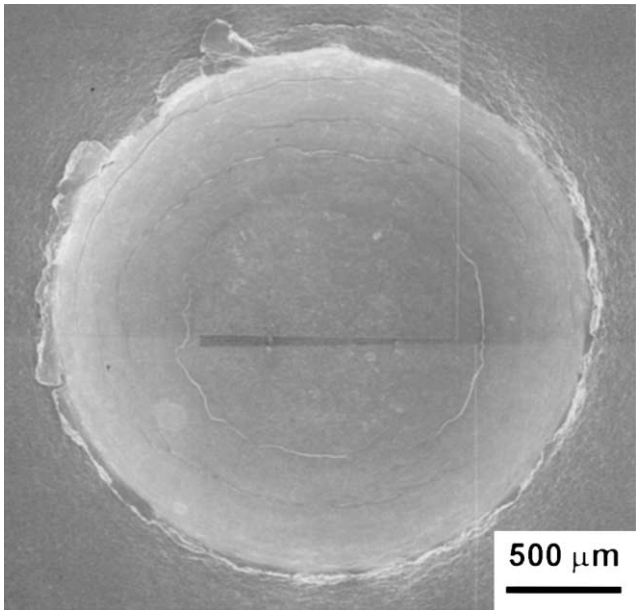

Fig. 2. SEM micrograph of 300 m s^{-1} impact crater.

(so-called K_B) specimens, at a velocity of 300 m s^{-1} using a compressed-gas gun facility (see [5]).

The effect of foreign-object damage on the fatigue behavior was examined using modified K_B specimens (cross section 3.2×5.2 mm, gauge length 20 mm). After impact, specimens were subsequently cycled (sinusoidal waveform) at nominally maximum stress levels of 225–500 MPa ($R = \sigma_{min}/\sigma_{max} = 0.1$). Throughout fatigue testing, specimens were periodically removed from the test frame and the progress of crack initiation and growth examined in a scanning electron microscope (SEM).

Approximate local stress intensities for small cracks at the indentation rim, were calculated from Lukáš' solution [6] for small cracks at notches (which includes indentation geometry and stress concentration effects), in terms of the crack depth a, indentation radius ρ, stress range $\Delta\sigma$, and elastic stress-concentration factor $k_t = 1.25$ [7]:

$$\Delta K = \frac{0.7k_t}{\sqrt{1 + 4.5(a/\rho)}} \Delta\sigma\sqrt{\pi a} \quad (1)$$

3. Results and discussion

3.1. Characterization of foreign-object damage

A typical damage site caused by 300 m s^{-1} impact is displayed in Fig. 2. Earlier results [5], showed that at velocities above 250 m s^{-1}, a pronounced pile-up of material (Fig. 2) at the crater rim resulted in multiple micro-notches and microcracking (insert in Fig. 3). When these microcracks (~ 2–25 μm) were favorably oriented with respect to applied stress axis on subsequent fatigue cycling, they were found to provide the nucleation sites for high-cycle fatigue-crack growth (Fig. 3).

3.2. Fatigue properties

Stress-life (S-N) data in Fig. 4 clearly show the detrimental effect of FOD on the fatigue strength. Specifically, at a far-field maximum stress of 500 MPa ($R = 0.1$), representing the 10^7-cycle fatigue limit for undamaged material, final failure in the damaged material occurred at approximately 4–5×10^4 cycles. As discussed earlier [5], this reduction in fatigue strength can be considered principally in terms of earlier fatigue crack initiation due to four prominent factors: (i) FOD-induced microcracking, (ii) stress concentration, (iii) residual stresses, and (iv) damaged microstructure.

It was found that the location for crack initiation at impact damaged sites depends strongly on impact velocity. Typically for 300 m s^{-1} impacts, FOD-induced microcracking in the pile-up region of the impact crater

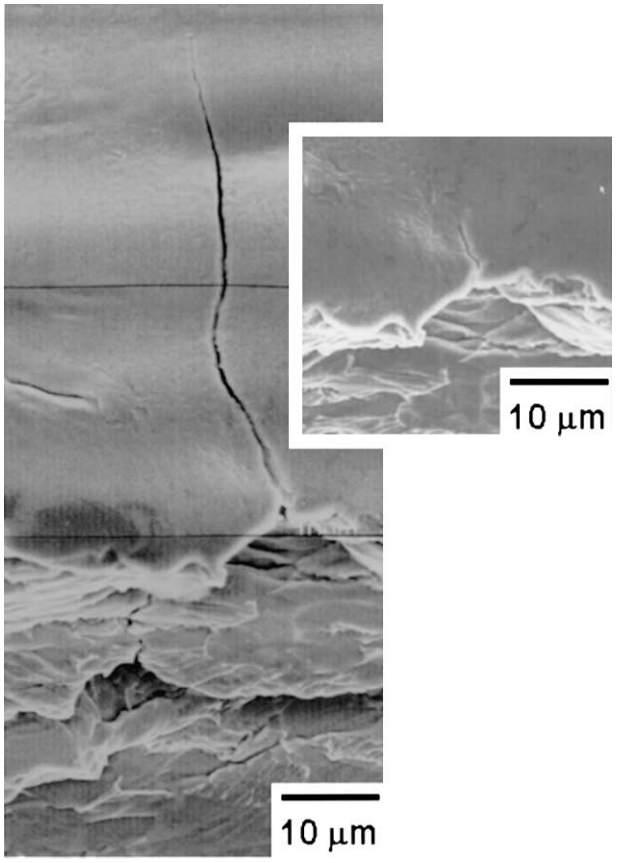

Fig. 3. SEM micrograph of FOD-induced microcracking at the crater rim (insert) and subsequent fatigue-crack growth at such microcrack after 29 000 cycles ($\sigma_{max} = 500$ MPa, $R = 0.1$).

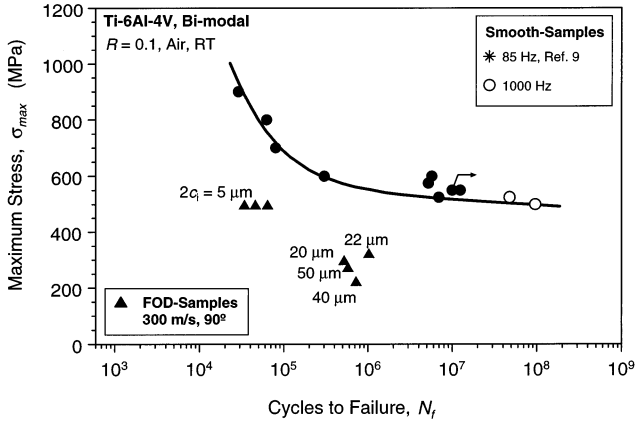

Fig. 4. S–N data show reduced fatigue life due to simulated FOD as compared with smooth-bar specimens [9] in bimodal Ti–6Al–4V. $2c_i$ is the surface crack length of FOD-induced microcracks.

rim provides the dominant site for the initiation of fatigue cracks on subsequent cycling (Fig. 3). For lower velocity impacts (200 m s^{-1}), no such microcracking could be detected; in this instance, surface cracks tended to form at the base of the indentation site where the stress concentration was highest [5]. This strongly implies that low velocity or quasi-static indentations do not necessarily provide a realistic simulation of FOD. In addition, tensile residual hoop stresses (estimated in [8]), the highly deformed microstructure in this region [5], and the stress-concentration factors ($k_t \sim 1.25$) are contributing factors.

Fig. 5 shows the fatigue-crack growth rates of FOD samples as compared with results of naturally-initiated small cracks (~ 45–1000 μm) [9], and through-thickness large cracks (> 5 mm) [2] in undamaged material. FOD-initiated small-crack growth rates are aligned approximately between the large-crack data (lower bound) and naturally-initiated crack data (upper bound). Typical for the small-crack effect e.g. [10], the growth rates of the naturally- and FOD-initiated small cracks are roughly in order of a magnitude faster than corresponding large-crack results at near-threshold levels. The large-crack threshold of ~ 1.9 MPa$\sqrt{m}$ at $R = 0.95$ (where the effect of crack closure is eliminated) is considered to be a definitive lower bound 'worst-case' threshold for cracks of dimensions large compared with the scale of the microstructure, i.e. for 'continuum-sized' cracks, as discussed earlier [2]. However, smallest FOD-initiated cracks (~ 2–25 μm), com-

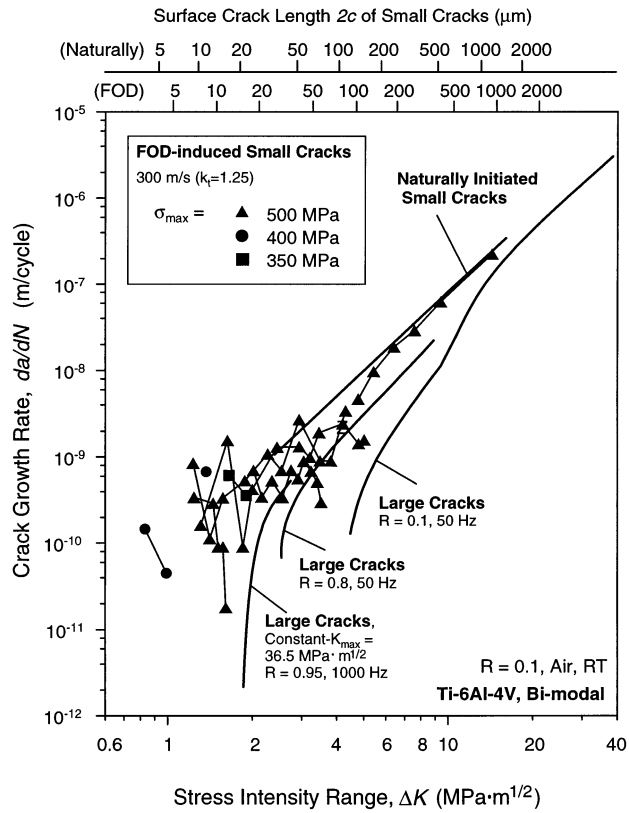

Fig. 5. Crack-growth rates as a function of applied stress-intensity range of FOD- and naturally-initiated small cracks and through-thickness large cracks in bimodal Ti–6Al–4V. Small-cracks were initiated at $\sigma_{max} = 650$ MPa ($R = -1$). [9] Large-crack growth data for $R \leq 0.8$ were derived from constant load-ratio tests, whereas for $R \geq 0.8$, constant-K_{max}/increasing-K_{min} testing was used [2].

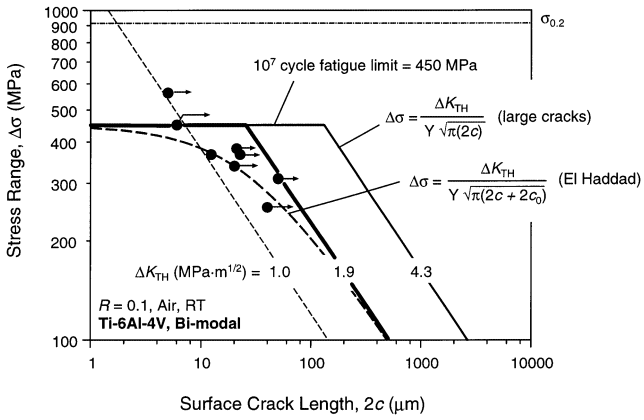

Fig. 6. Crack growth conditions of FOD-induced small-cracks ($da/dN = 10^{-11}$–10^{-10} m per cycle) as a function of cyclic stress range and surface crack length are shown in a modified Kitagawa–Takahashi diagram.

parable with microstructural size-scales, can propagate at stress intensities well below this 'worst-case' threshold. This is specifically at applied stress intensities as low as $\Delta K \sim 1$ MPa$\sqrt{\text{m}}$, at nominal maximum stresses from 325 to 500 MPa ($R = 0.1$), presumably due to biased sampling of the 'weak links' in the microstructure. It is believed that a ΔK of 1 MPa$\sqrt{\text{m}}$ is the lowest stress-intensity range ever measured for crack growth in Ti–6Al–4V. It should be noted here that although the FOD-induced residual stresses are not included in the calculation of K (Eq. (1)), such stresses do not change the stress-intensity range (ΔK); they affect the mean stress and hence, alter the local load ratio. It is clear that the earlier stated argument [2,5] for the notion of a high-cycle fatigue threshold, which was based on the concept of a 'worst-case' threshold (determined under $R \rightarrow 1$ conditions that minimize crack closure), applies strictly for 'continuum-sized' cracks. It does not provide a lower-bound threshold stress intensity for cracks on the scale of microstructural dimensions, as in the earliest stages of FOD-induced fatigue failure.

Coupling the notion of the 'worst-case' threshold stress intensity with the fatigue limit, as in the Kitagawa–Takahashi diagram [11], provides an alternative approach to defining limiting conditions for HCF and FOD-related damage. Fig. 6 shows the influence of crack size on the fatigue thresholds in the form of a modified Kitagawa diagram for crack-growth threshold conditions of $da/dN = 10^{-11} - 10^{-10}$ m per cycle. According to this approach (solid line), the stress range $\Delta\sigma$ for crack arrest is defined by the 10^7-cycle fatigue limit with the fatigue-crack growth threshold (ΔK_{TH}) measured on 'continuum-sized' cracks. El Haddad et al. [12] empirically quantified the threshold conditions by introducing a constant (intrinsic) crack length $2c_0$, such that the stress intensity is defined as $Y\Delta\sigma\sqrt{\pi(2c + 2c_0)}$, where Y is the geometry factor.

The present results, plotted in this format in Fig. 6, show that crack growth from FOD-induced microstructurally-small cracks apparently occur at stress concentration corrected stress ranges well predicted by the Kitagawa–El Haddad limit, defined by the 'worst-case' ΔK_{TH} threshold and 10^7-cycle fatigue limit.

4. Conclusions

Simulated FOD impact (300 m s^{-1}) of steel spheres on a flat surface markedly degrade fatigue strength of Ti–6Al–4V. Specifically, the fatigue life of smooth-bar samples was reduced by some two orders of magnitude at an applied stress corresponding to the smooth-bar 10^7-cycles fatigue limit ($R = 0.1$).

The detrimental effect of FOD is attributed to (i) FOD-induced precracks at the crater rim of the damaged zone, (ii) stress concentration associated with the FOD indentation, (iii) presence of tensile residual stresses at the crater rim and (iv) microstructural damage due to FOD-impact.

The principal effect of FOD in reducing fatigue life was found to induce microcracks in the pile-up of material around the impact crater rim, i.e. preferred sites for the premature initiation of fatigue cracks.

At far-field maximum stresses from 325 to 500 MPa ($R = 0.1$), FOD-initiated cracks ($\sim$2–25 μm) grow at applied stress intensities as low as $\Delta K = 1$ MPa$\sqrt{\text{m}}$, i.e. well below the 'worst-case' ΔK_{TH} threshold of 1.9 MPa$\sqrt{\text{m}}$ for 'continuum-sized' cracks (cracks larger than the characteristic microstructural size-scales) in this alloy.

Correspondingly, the critical condition for HCF in the bimodal Ti–6Al–4V in the presence of 'continuum-sized' cracks ($>$ 50–100 μm) can be defined in terms of the 'worst-case' fatigue threshold (determined under $R \rightarrow 1$ conditions that minimize crack closure).

However, the preferred approach for FOD-initiated failures in the presence of microstructurally-small cracks is to use the modified Kitagawa–Takahashi diagram, where the limiting conditions for HCF are defined in terms of the stress concentration corrected 10^7-cycle fatigue limit (at microstructurally-small cracks sizes) and the 'worst-case' ΔK_{TH} fatigue threshold (at larger, 'continuum-sized' crack sizes).

Acknowledgements

This work was supported by the Air Force Office of Science and Research, Grant No. F49620-96-1-0478, under the Multidisciplinary University Research Initiative on 'High Cycle Fatigue' to the University of California, Berkeley. Special thanks are due to Professor Werner Goldsmith (UCB) for providing the com-

pressed-gas gun facility, and to Professor J. W. Hutchinson, B. L. Boyce, Dr J. M. McNaney and Dr A. W. Thompson for helpful discussions.

References

[1] J.R. Larsen, B.D. Worth, C.G. Annis Jr, F.K. Haake, Int. J. Fracture 80 (1996) 237–255.
[2] R.O. Ritchie, D.L. Davidson, B.L. Boyce, J.P. Campbell, O. Roder, Fatigue Fract. Eng. Mat. Struct. 22 (1999) 621–631.
[3] T. Nicholas, J.R. Barber, R.S. Bertke, Experiment. Mech., (1980), pp. 357–364.
[4] S.J. Hudak, K.S. Chan, R.C. McClung, G.G. Chell, Y.-D. Lee, D.L. Davidson, High Cycle Fatigue of Turbine Blade Materials, Final Technical Report UDRI Subcontract No. RI 40098X SwRI Project No. 18-8653, 1999.
[5] J.O. Peters, O. Roder, B.L. Boyce, A.W. Thompson, R.O. Ritchie, Metall. Mater. Trans. 31A (2000) 1571–1583.
[6] P. Lukáš, Eng. Fract. Mech. 26 (1987) 471–473.
[7] M. Nisida, P. Kim, Proceedings of the Twelfth National Congress on Applied Mechanics, 1962, pp. 69–74.
[8] X. Chen, J.W. Hutchinson, Int. J. Fract., 2000, in press.
[9] J.A. Hines, J.O. Peters, G. Lütjering, in: R.R. Boyer, D. Eylon, G. Lütjering (Eds.), Fatigue Behavior of Titanium Alloys, TMS, Warrendale, PA, 1999, pp. 15–22.
[10] R.O. Ritchie, J. Lankford, Mater. Sci. Eng. 84 (1986) 11–16.
[11] H. Kitagawa, S. Takahashi, Proceedings of Second International Conference on Mechanical Behavior of Materials, ASM, Metals Park, OH, 1976, pp. 627–631.
[12] M.H. El Haddad, T.H. Topper, K.N. Smith, Eng. Fract. Mech. 11 (1979) 573–584.